Radio and X-ray diagnostics of flare accelerated electrons

during the commissioning phase of Solar Orbiter

David Paipa

Advisors:
Dr. Milan Maksimovic
Dr. Nicole Vilmer

LESIA
l'Observatoire de Paris | PSL

PNST 2024 - Marseille
January 10, 2024

Energetic particles in solar flares: Particle acceleration and transport

Release of the free magnetic energy contained in **complex** magnetic fields can occur through the process of **magnetic reconnection**

electrons escaping through open magnetic field lines

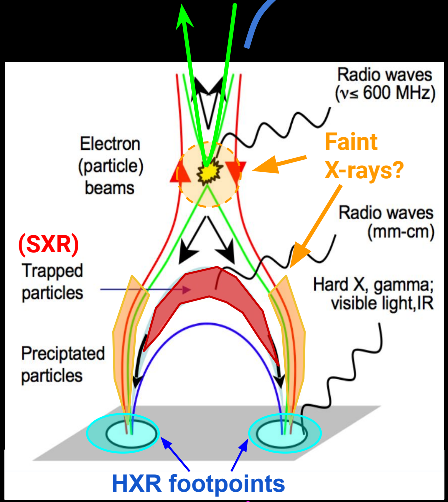

Adapted from Klein, 2006

electrons fall back into the chromosphere

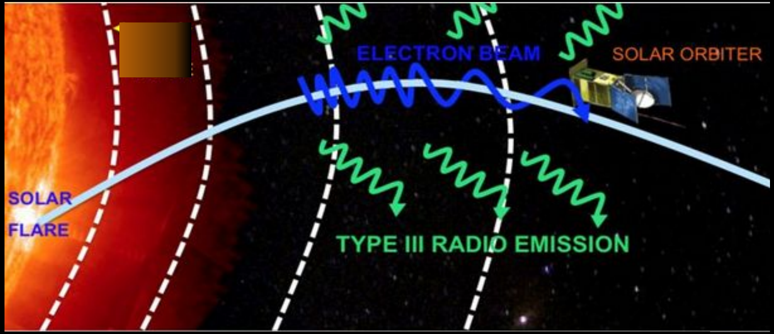

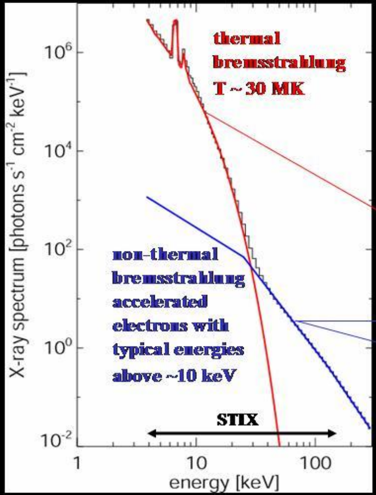

HXR emission of a solar flare

RHESSI observations: Thermal and non-thermal components

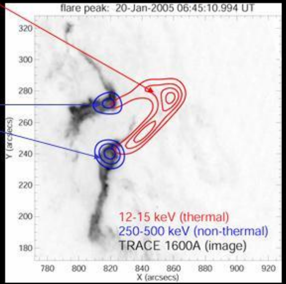

Plasma emission mechanism

Radio emissions in IP medium

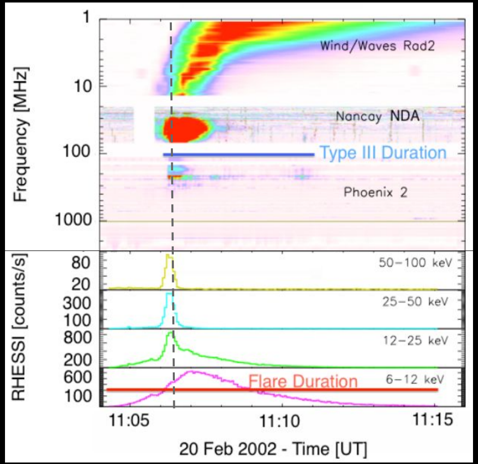

Adapted from Reid & vilmer, 2016

HXR emissions in the chromosphere

Bremsstrahlung

Context on Radio/X-ray observations

The timing of main HXR peak and Radio emissions can be very similar . . .

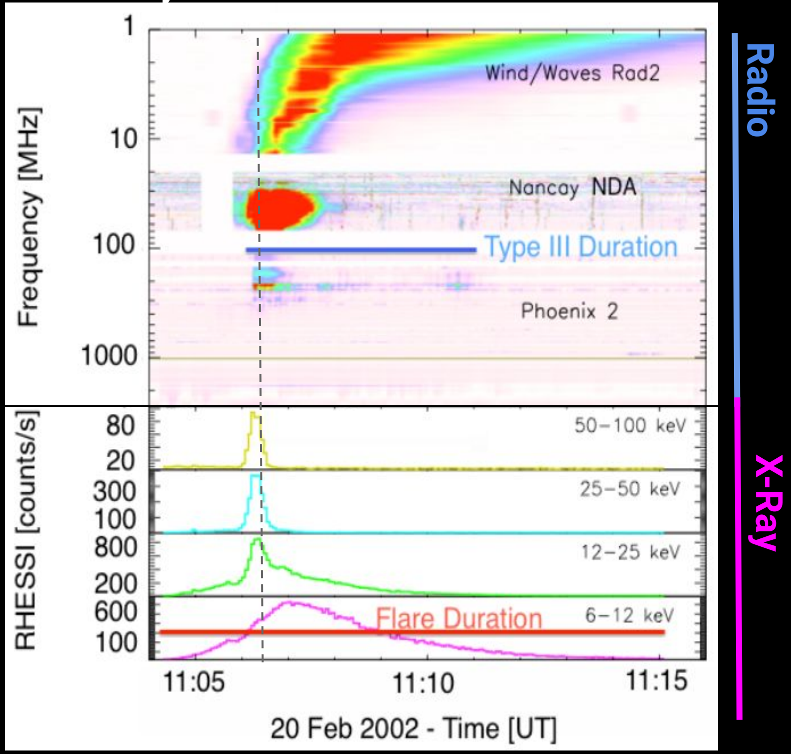

. . . BUT this is not always the case

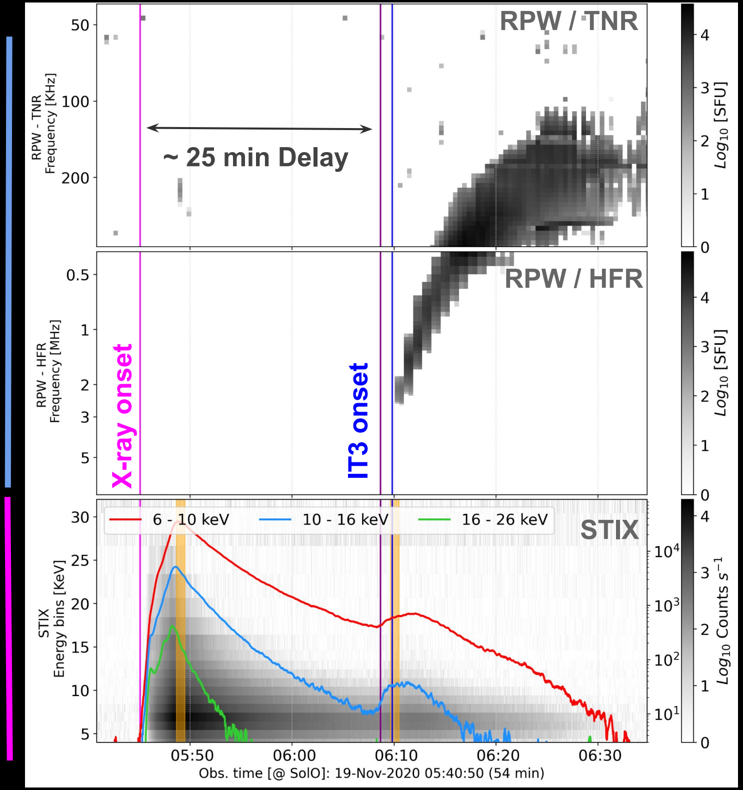

Context on Radio/X-ray observations: IPT3 delayed emission

The timing of main HXR peak and Radio emissions can be very similar . . .

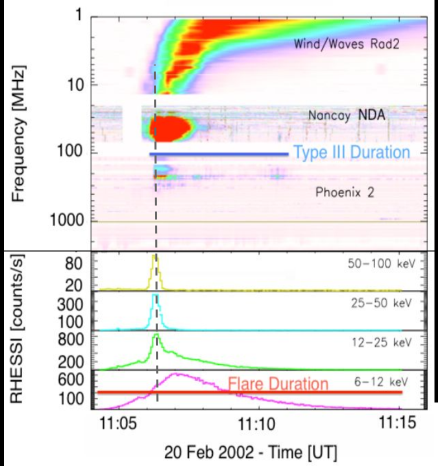

Radio

X-Ray

Co-temporal X-ray/IP radio emissions

simple scenario

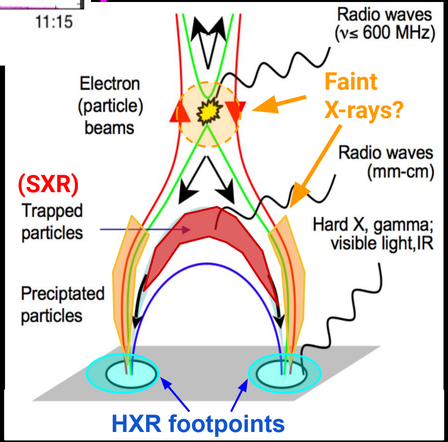

. . . BUT this is not always the case

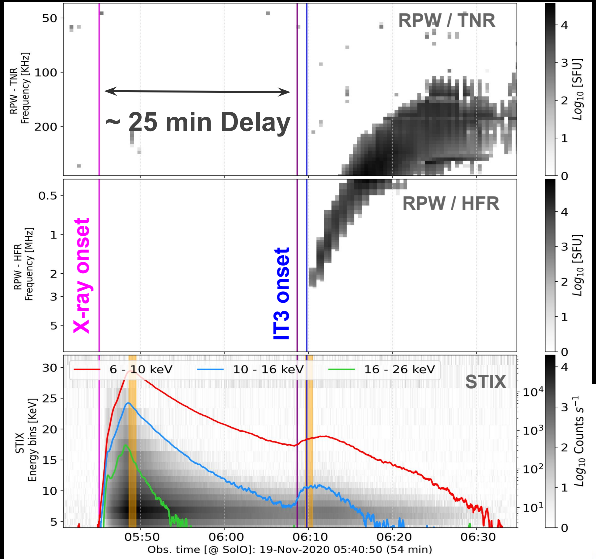

emissions w.r.t. X-ray onset

more complex scenarios
e.g. Interchange reconnection.

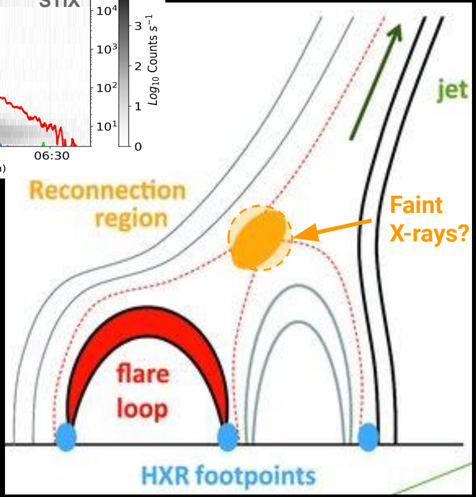

Context on Radio/X-ray observations: Previous studies

Previous statistical studies characterizing the correlation between HXR and radio emission intensities

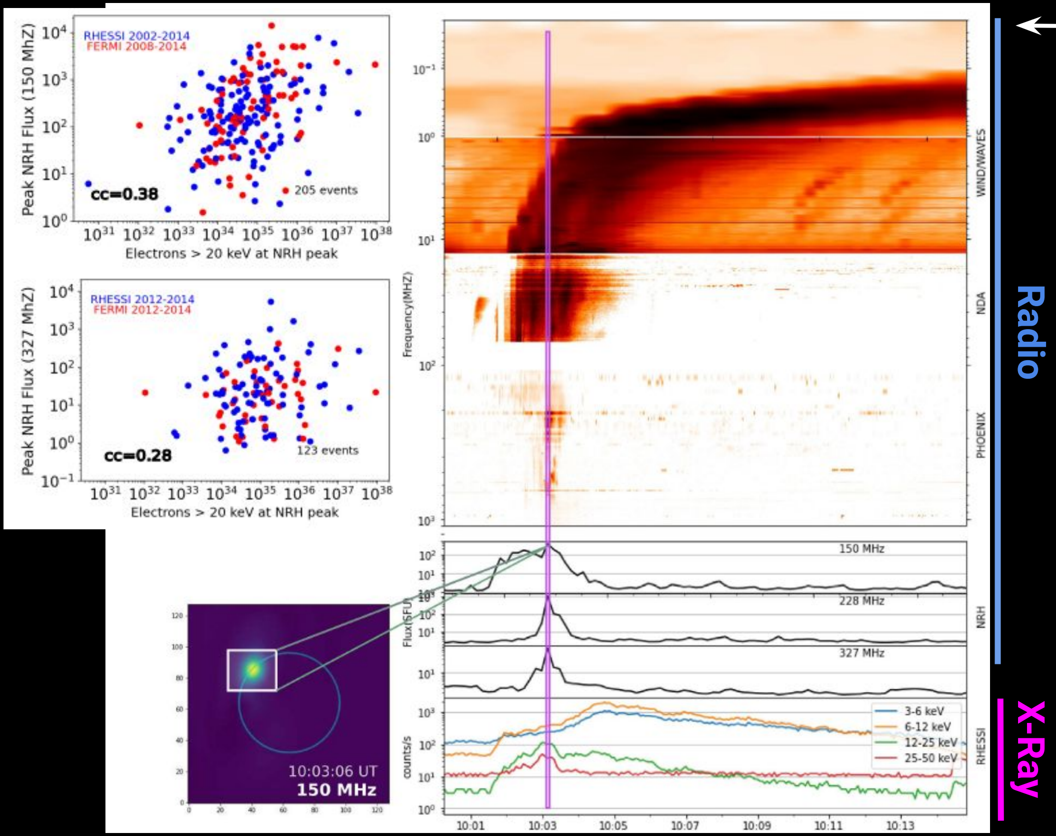

James, vilmer 2023
Correlation between non-thermal electron number with E > 20 keV at HXR peak vs. peak NRH flux at different frequencies

~200 events analyzed in **13 year interval**

Combining observations from different observatories **limits the number of events**

Fortunately . . .

Solar Orbiter observes in X-ray and Radio **from the same platform**

The Solar Orbiter

Launched in February 2020
Getting as close as ~0.28 AU
10 instruments onboard

- 4 in-situ
- 6 remote sensing

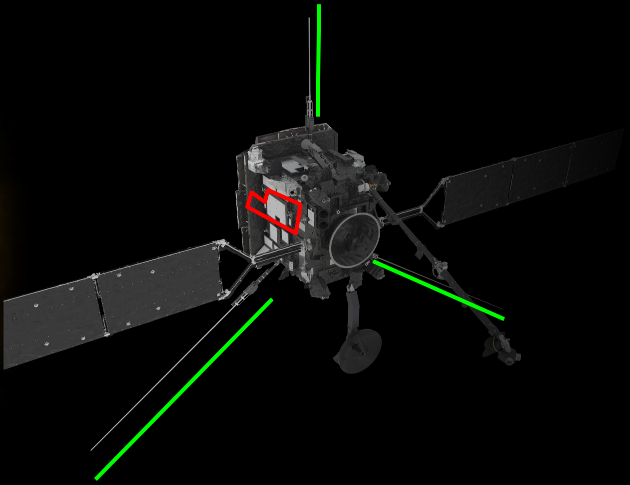

STIX

Spectrometer/telescope for imaging X-rays

- **Energy range:** 4 to 150 keV
- X-ray remote sensing
  - **bi-grid imaging (Indirect)**
  - spectroscopy

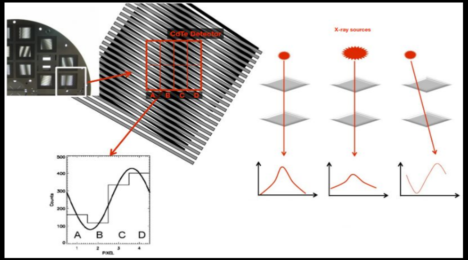

RPW

Radio and Plasma Waves Instrument

- 3 antennas , Radio waves measurements
- **Frequency range: ~DC to 16.4MHz**

How do solar eruption produce energetic particle radiation that fills the heliosphere?

First available interval for STIX/RPW combined observations between 17 and 21 November 2020

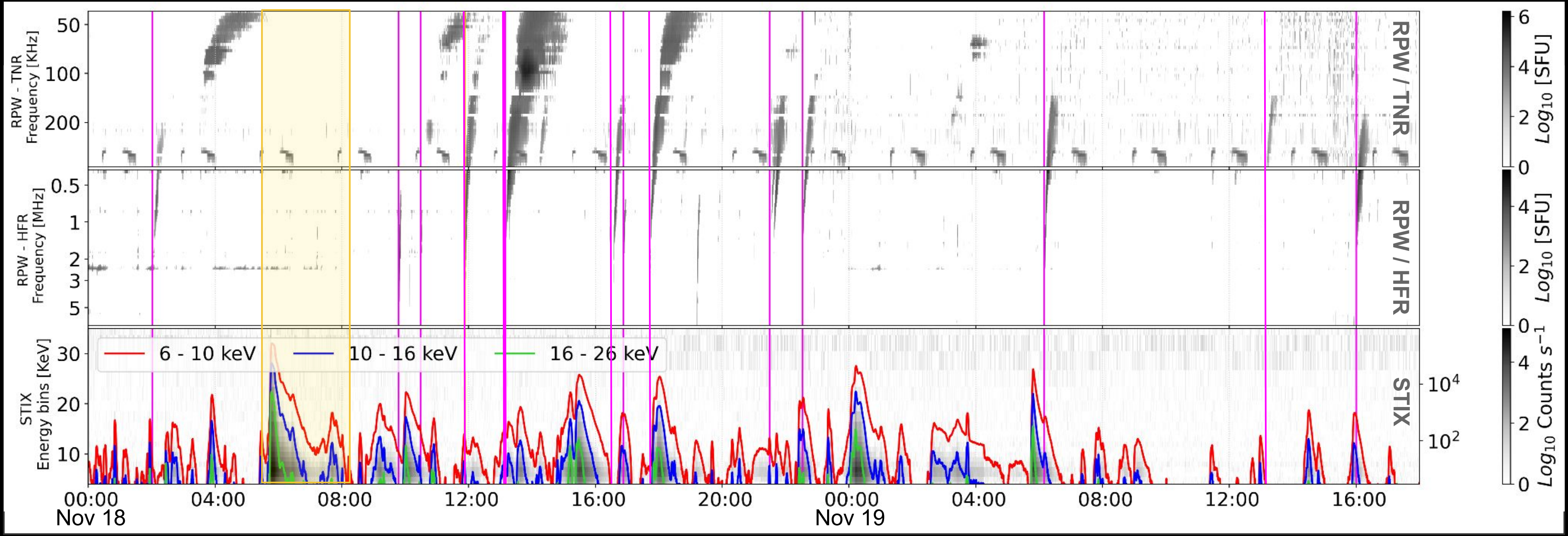

- Not all X-ray flares have an IPT3 associated, including some of the strongest flares
- Observation of intense IPT3s related to small flares

What conditions determine the presence of IPT3s in solar flares?

Case study: Observation of the November 2020 period

Events from **first available interval for STIX/RPW combined observations** between **17 and 21 November 2020**

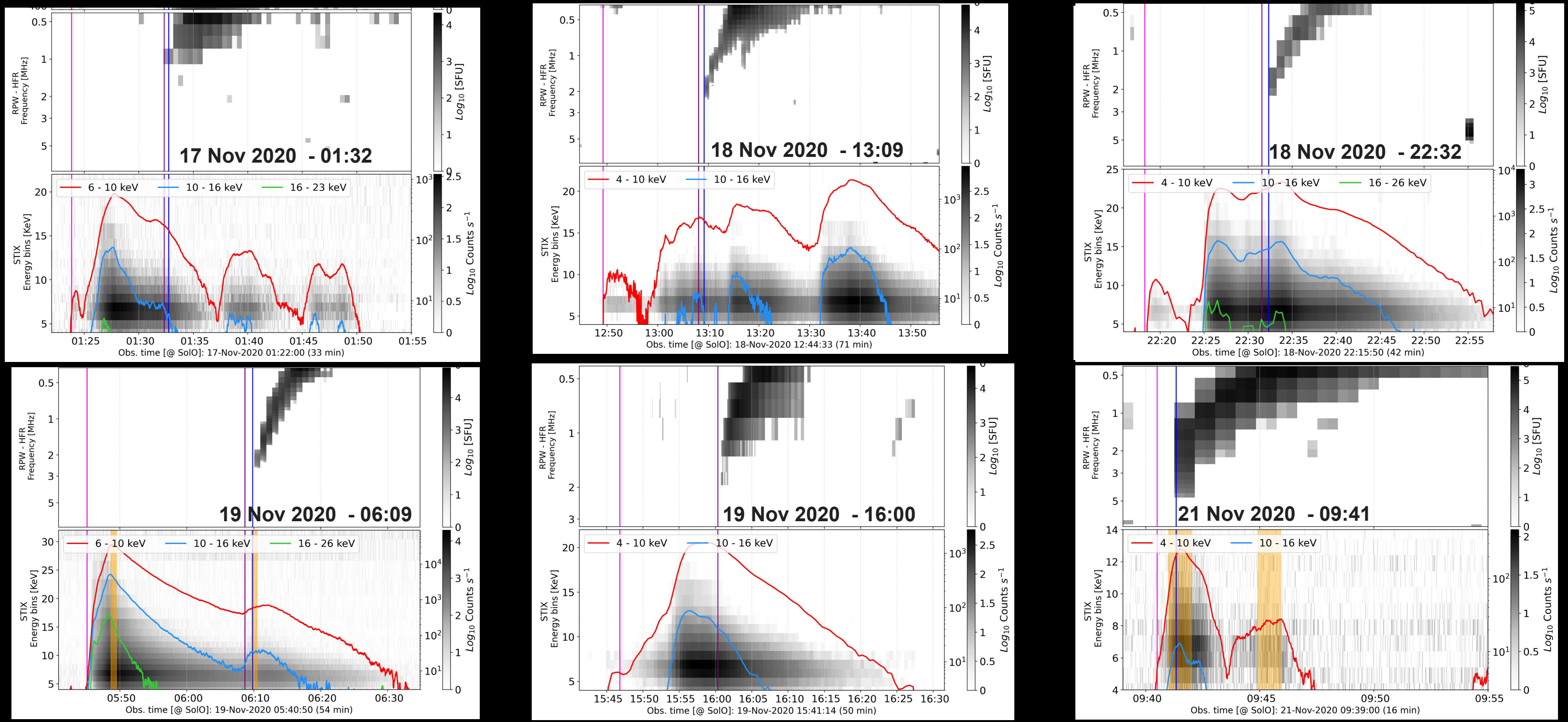

RPW/STIX data availability to study **15 flares with IPT3s associated**

UV images (EUI/FSI 174A) also available for some of them

Results: Active region

All of the 15 X-ray flares with IPT3s are located in the **same active region**

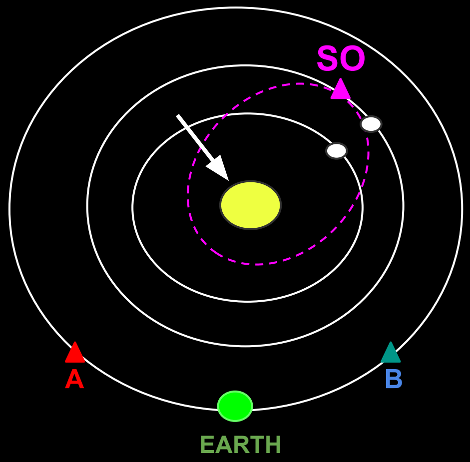

EUI/FSI 174A 18 Nov - 21:57

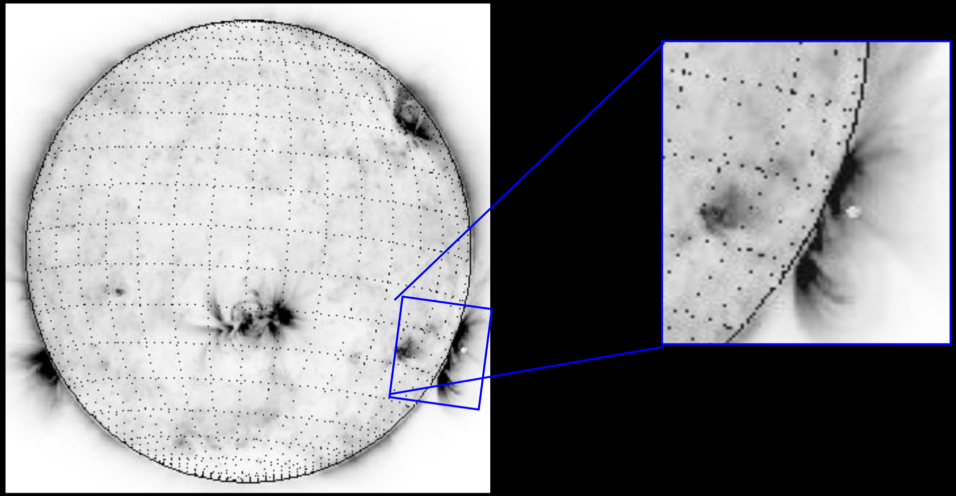

The Active region is transiting through the limb from Solar Orbiter's perspective

Results: Systematic imaging

17 Nov 2020 - IT3 time 01:32

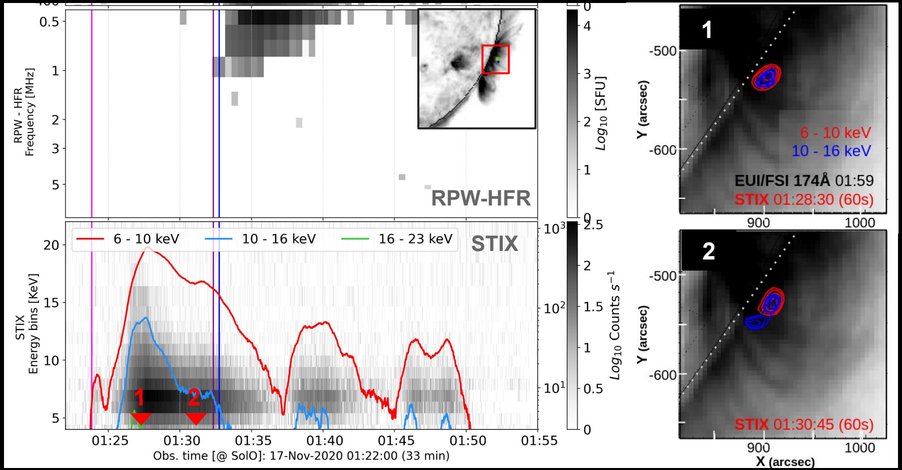

18 Nov 2020 - IT3 time 13:09

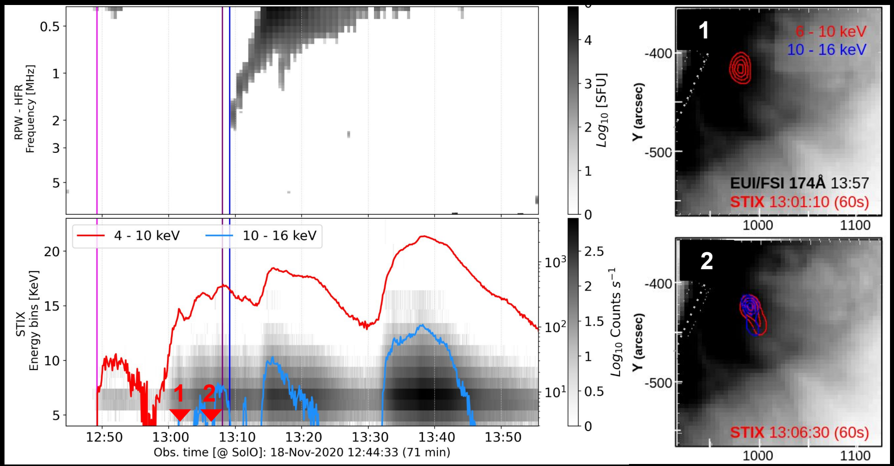

19 Nov 2020 - IT3 time 06:10

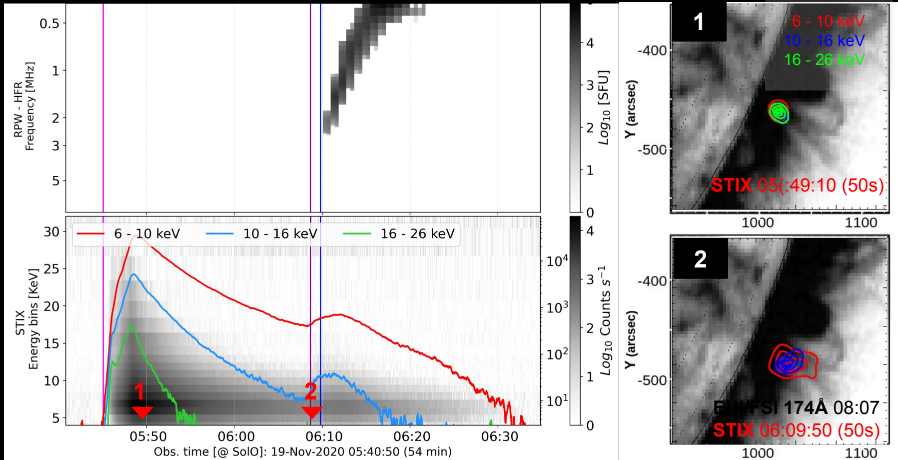

18 Nov 2020 - IT3 time 22:32

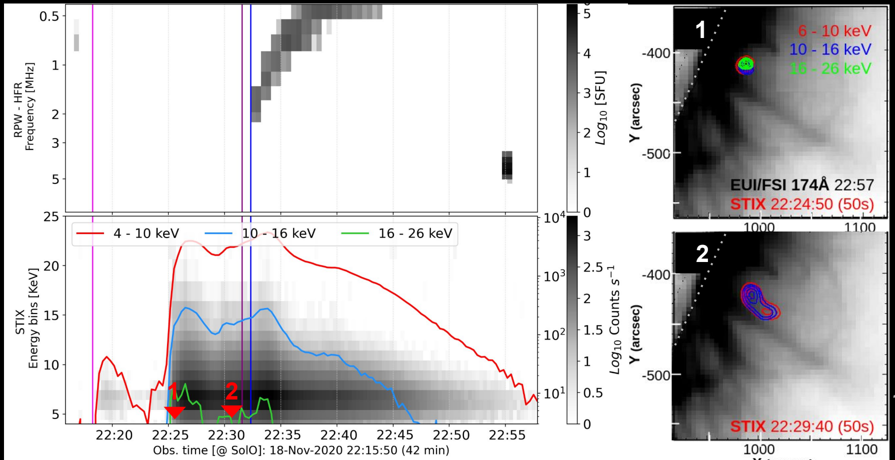

Results: Observations

Change in morphology of X-ray sources observed before/during IT3 onset time **for all 15 flares**

4 cases:

appearance of **new X-ray sources** before/during **IPT3 onset time**

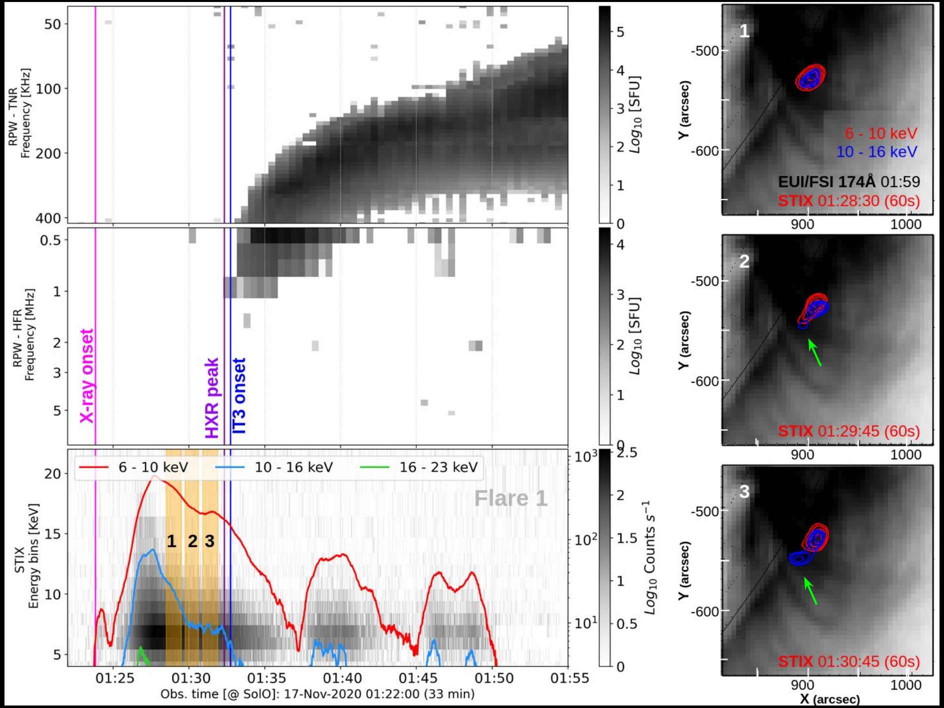

11 cases:

Change in the X-ray source shape before/during **IPT3 onset time**

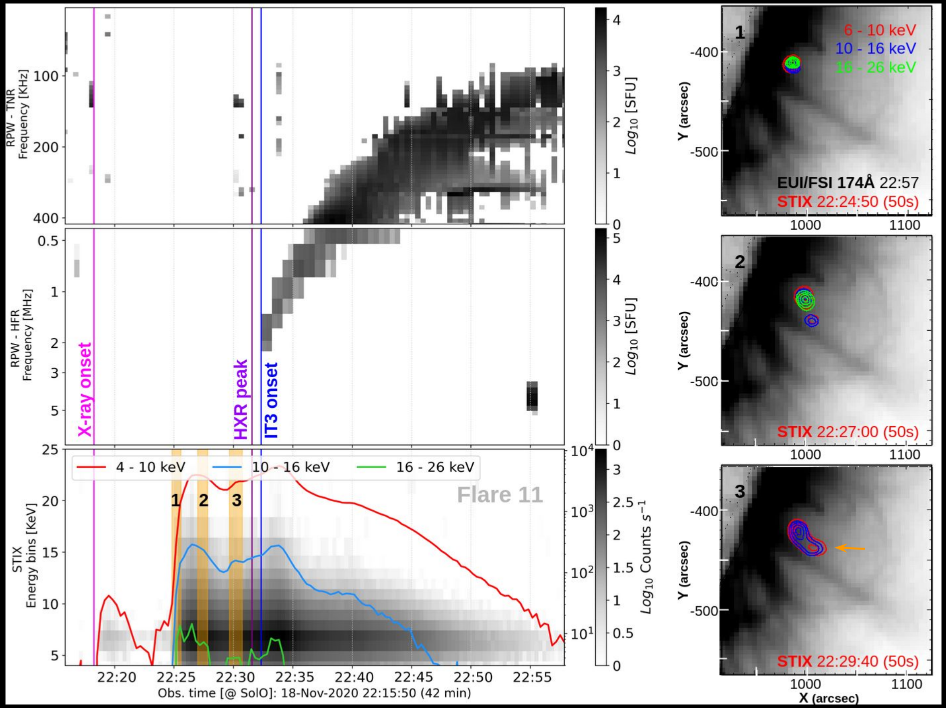

Results: Open magnetic field lines

8 cases:

X-ray sources **change morphology** close to the same “open-like” plasma structures before/during the **IPT3 onset time**

All the observed IPT3s within a 30h time lapse

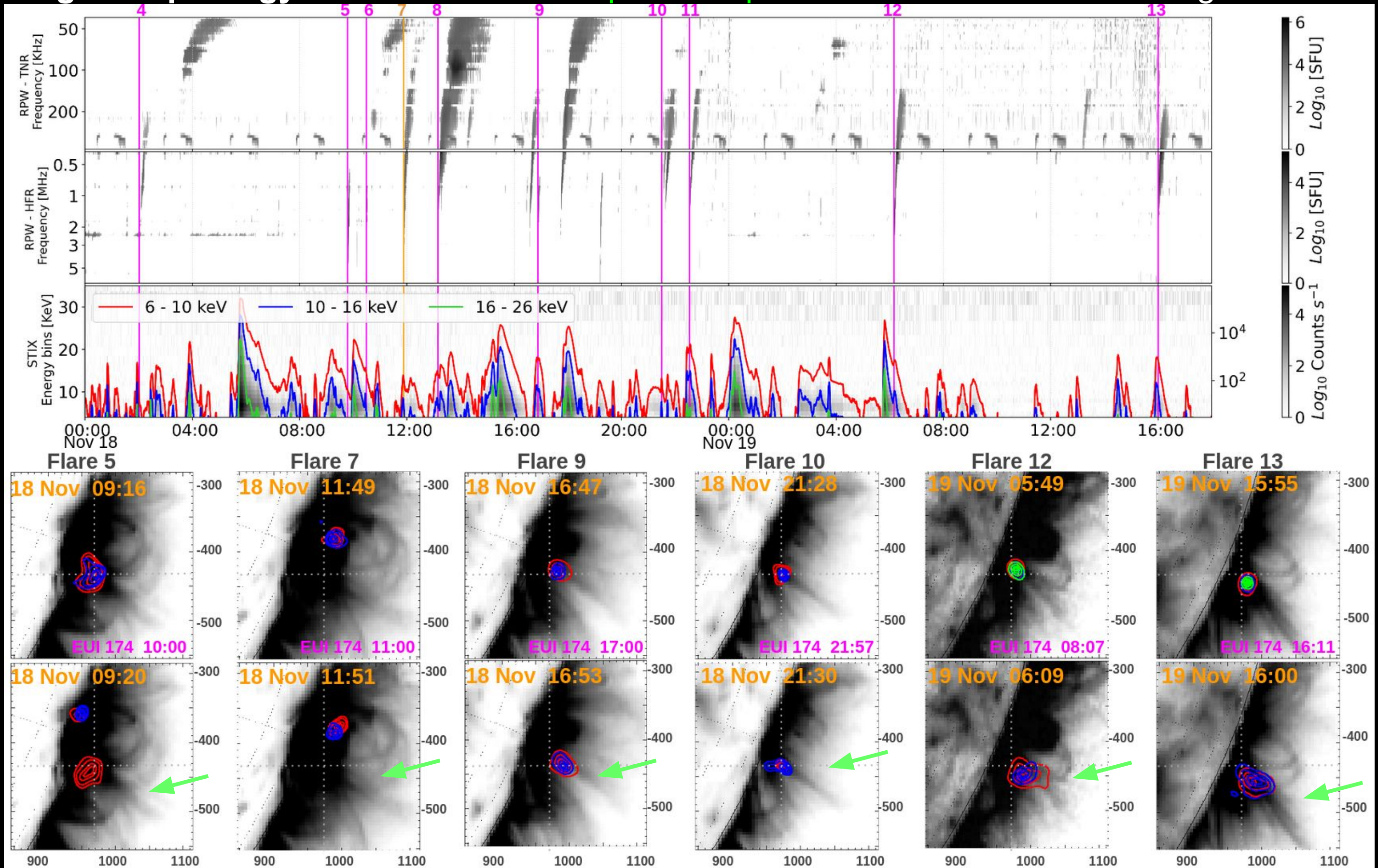

Before IPT3 onset

During IPT3 onset

Results: Open magnetic field lines

Running difference images in UV (1h difference) show emission enhancement in OMFL

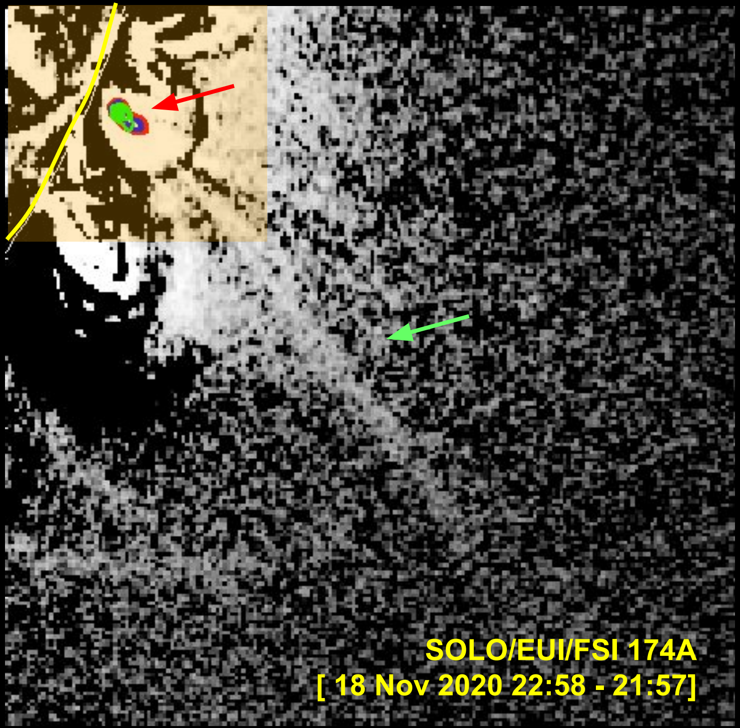

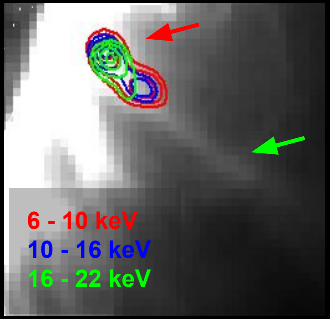

Elongation of X-ray sources towards OMFL

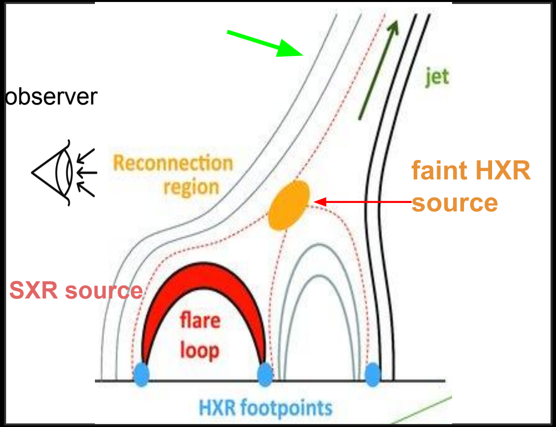

Adapted from Krucker, Kontar et al. 2011

Flares observed on the limb

Observed from “the side” given the vantage point of Solar orbiter

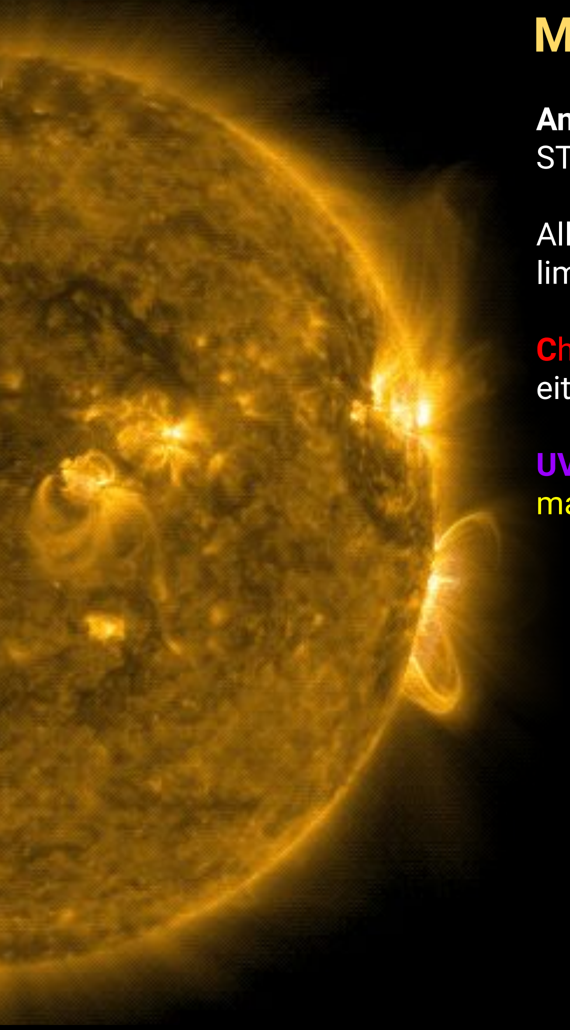

Main ideas to take home

Analysis of 15 flares with IPT3 associated during the first period with availability for STIX/RPW combined observations

All of them were located **close to the same active region,** transiting through and behind the limb in the observation period

Change in the x-ray source morphology close to the IPT3 onset time observed in all cases, either change in shape or new X-ray sources appear

UV images show that the HXR emission sites change morphology towards persistent open magnetic field lines.

Thanks :)

Questions? comments?

david.paipa@obspm.fr

ANNEX

Energetic particles in solar flares: Introduction

One of the main science objectives of Solar Orbiter

> How do solar eruption produce energetic particle radiation that fills the heliosphere?

The sun is a huge particle accelerator!

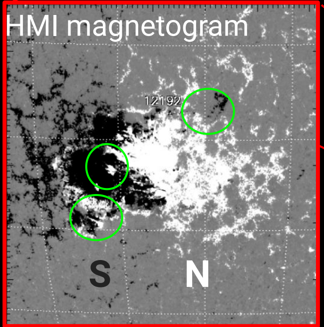

Complex magnetic field structure in **Active Regions (AR)**

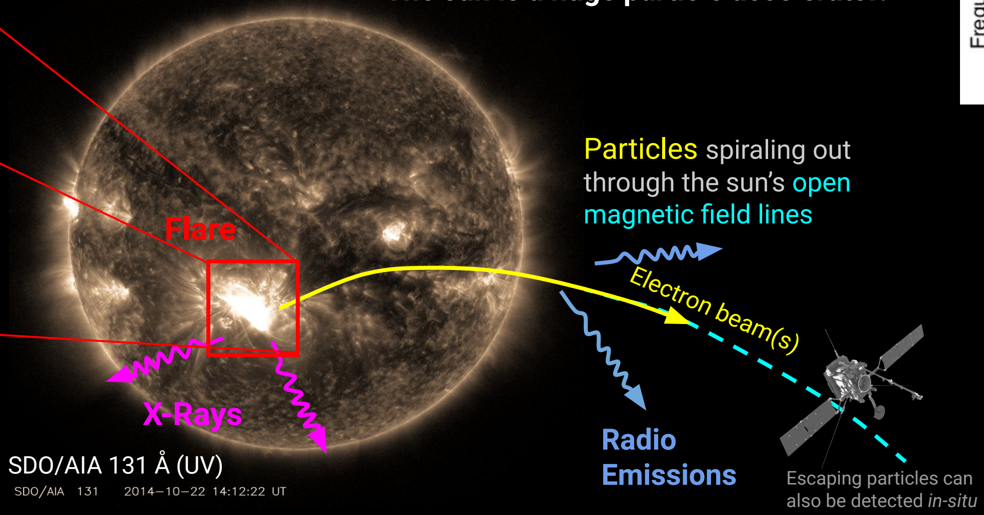

SDO/AIA 131 Å (UV)

Radio emissions drifting from high to low frequencies

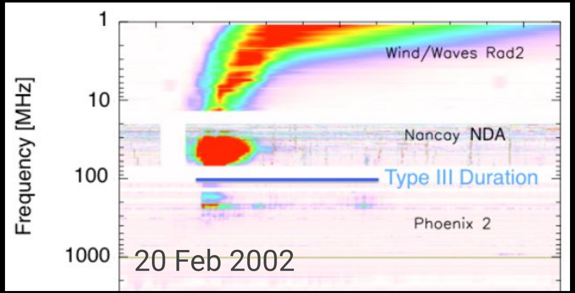

Enhancement in X-Ray emissions

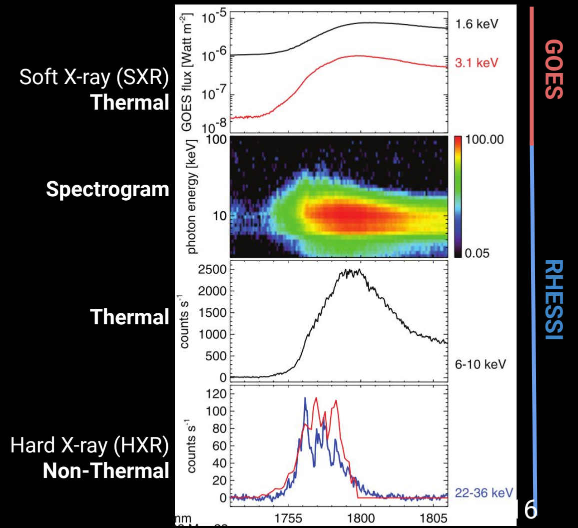

Magnetic energy is stored in non-potential fields → energy is released in ARs during solar flares →

- Plasma heating
- Particle acceleration
- Mass motions

Table 1. Summary of the X-ray flares and Interplanetary Type III bursts (IT3) observed by STIX and RPW, respectively, between 17 and 21 November 2021.

Day	Flares[a]	IT3[b]	IT3 (peak)[c]	sample IT3[d]	R[e]
17	81	6	6	3	1.00
18	59	13	9	7	0.69
19	33	4	3	2	0.75
20	21	4	1	1	0.25
21	38	5	1	1	0.20
Sum	232	32	21	15	0.66

Notes.

[a] Number of X-ray flares per day according to the STIX Data Center
[b] IT3s detected by RPW
[c] IT3s that can be associated with an HXR peak
[d] IT3s included in the study sample
[e] Ratio of association of detected IT3s with HXR peaks

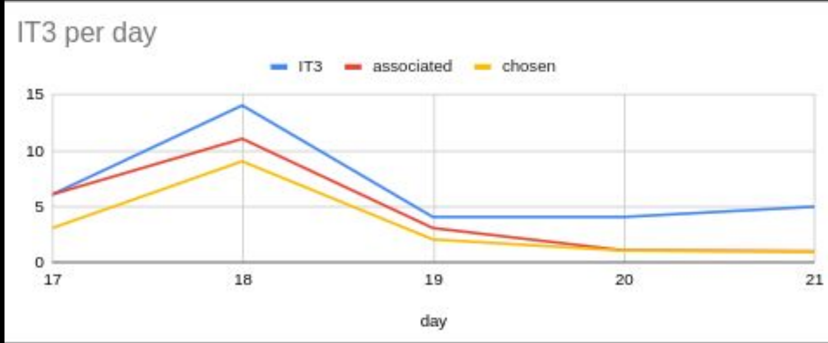

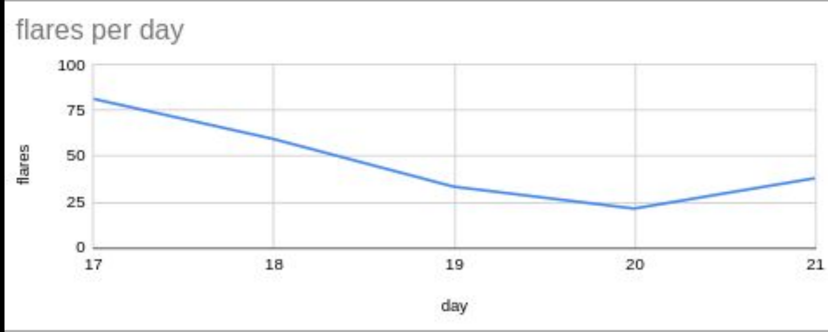

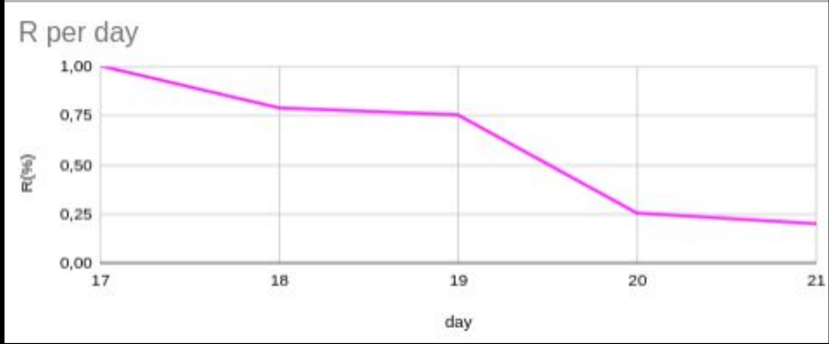

Results: Delays

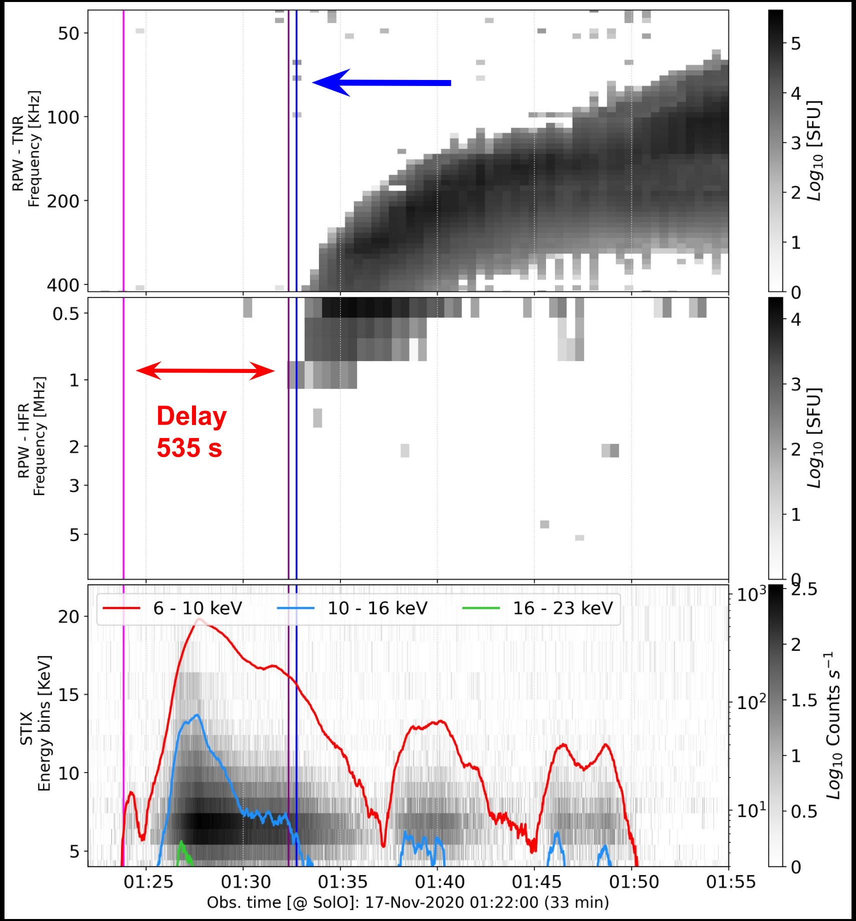

The delay of the IPT3 onset time with respect to the associated HXR peak is around 3 minutes (or less) for all flares

For only 6 cases the IPT3 is associated with the main HXR peak of the flare

For most of the cases the delay between the IPT3 onset time and the X-ray onset time is above 10 minutes

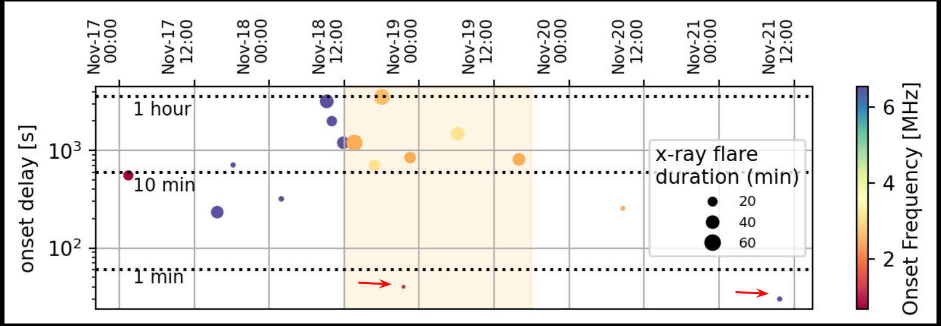

Method for X-ray and Radio Diagnostics: Nice example of delay in Type III bursts

Flare on July 17, 2021
UT 05:05

Presence of (IP) Type III bursts

Flare counts in energies up to 84 KeV

several impulsive HXR emission peaks, some of them temporally associated with IPT3s

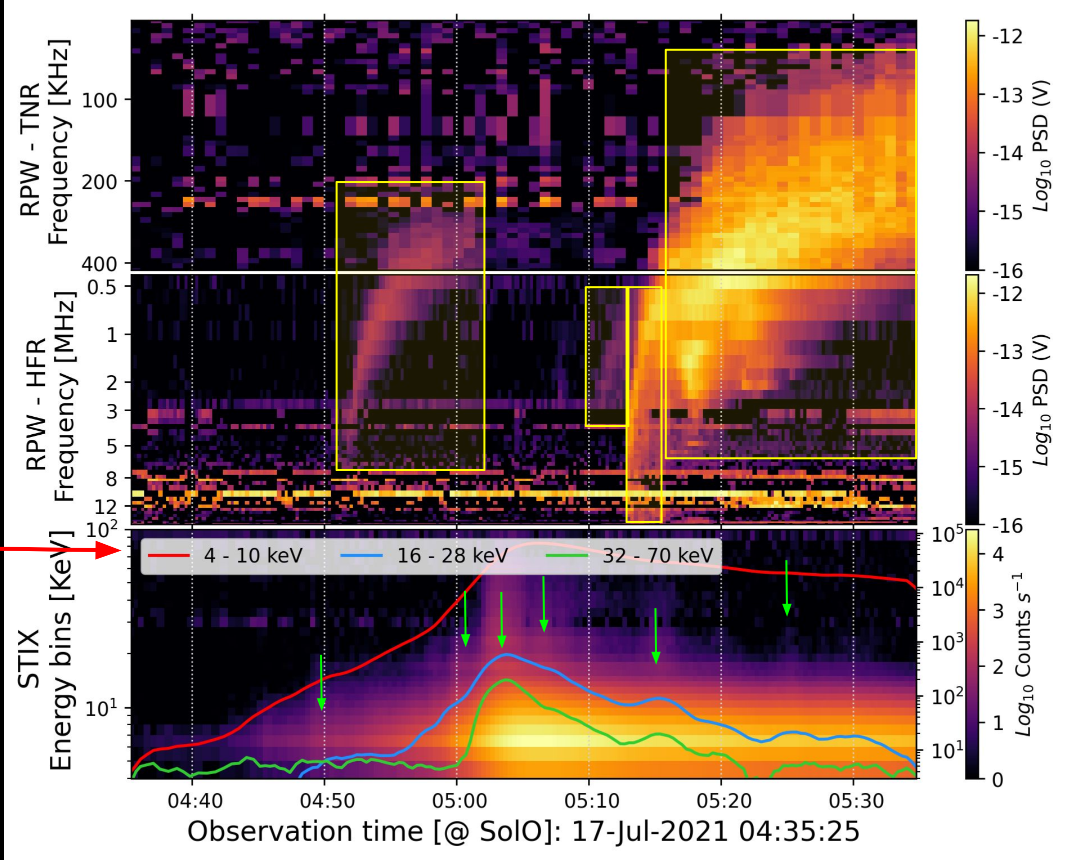

Method for X-ray and Radio Diagnostics: Nice example of delay in Type III bursts

Flare on July 17, 2021
UT 05:05

Presence of (IP) Type III bursts

Flare counts in energies up to 84 KeV

several impulsive HXR emission peaks, some of them temporally associated with IPT3s

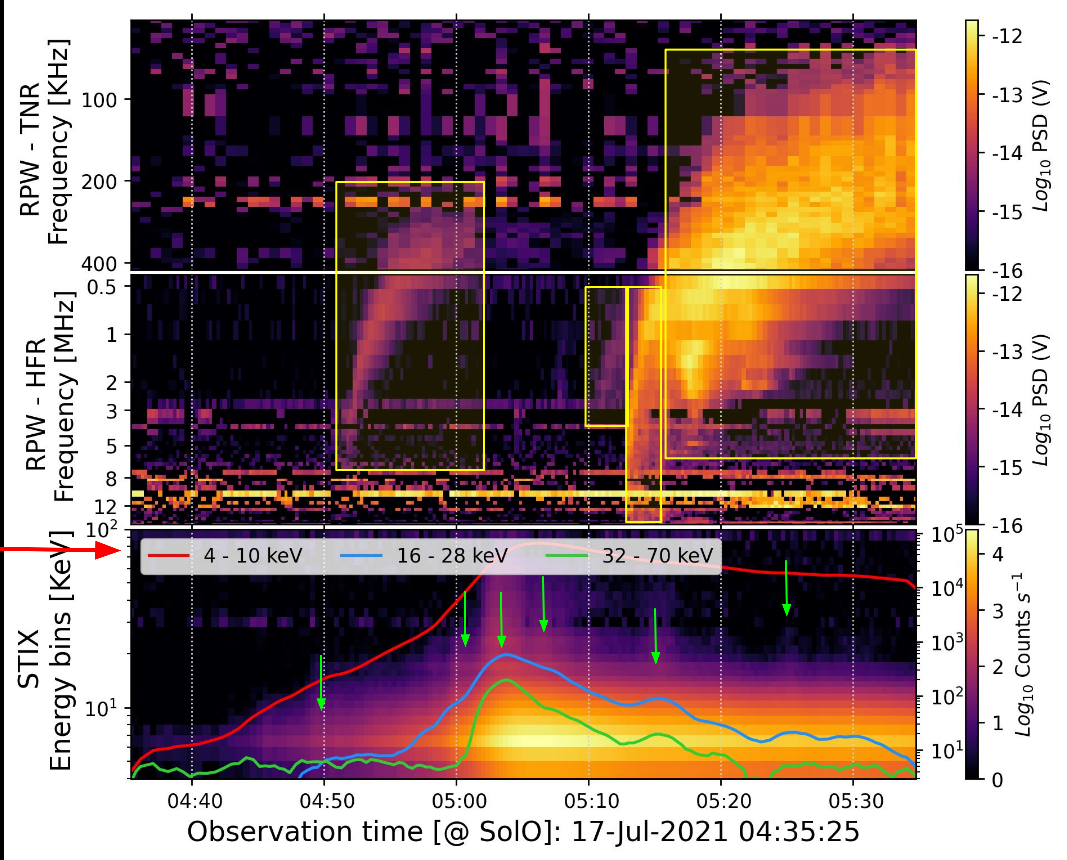

X-ray Diagnostics: Timing and Imaging

Imaging of 4 time intervals close to the IPT3 onset time (Before and during)

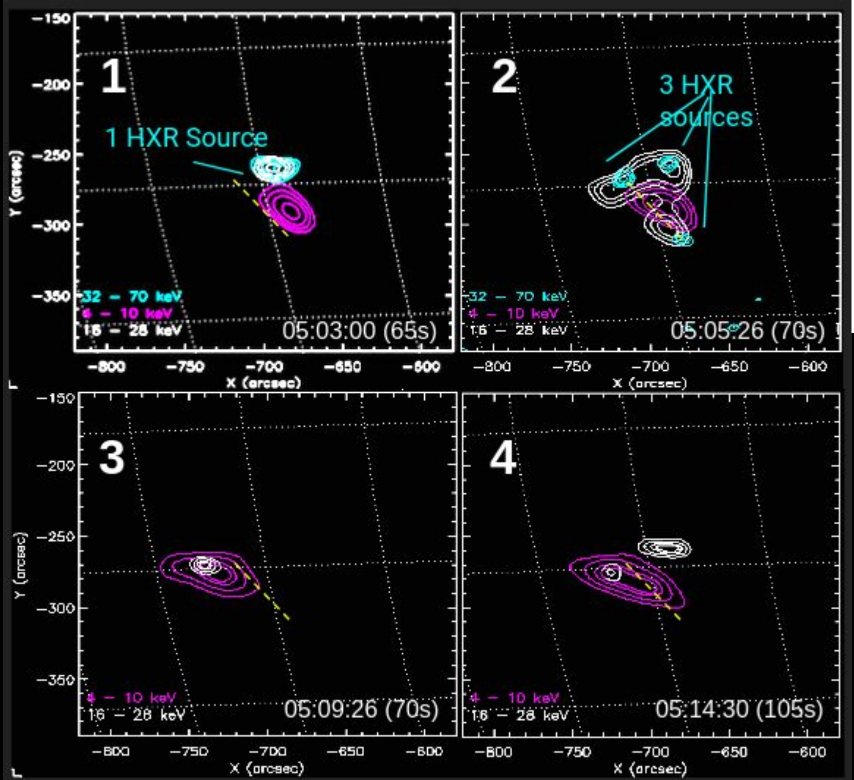

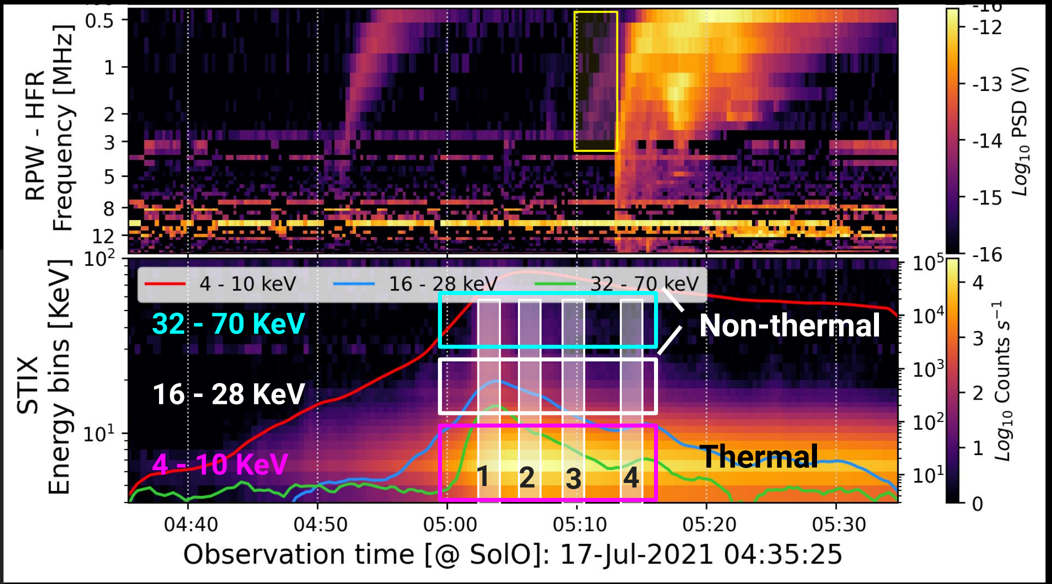

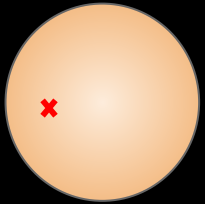

Flare position on solar disk

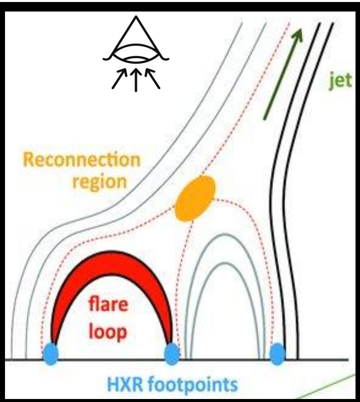

Adapted from Krucker, Kontar et al. 2011

X-ray Diagnostics: Spectroscopy

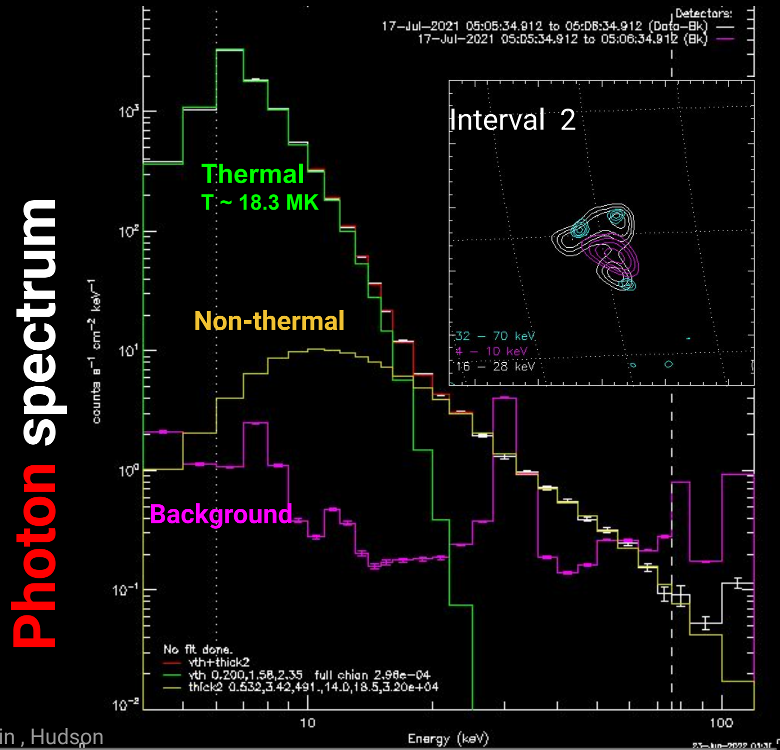

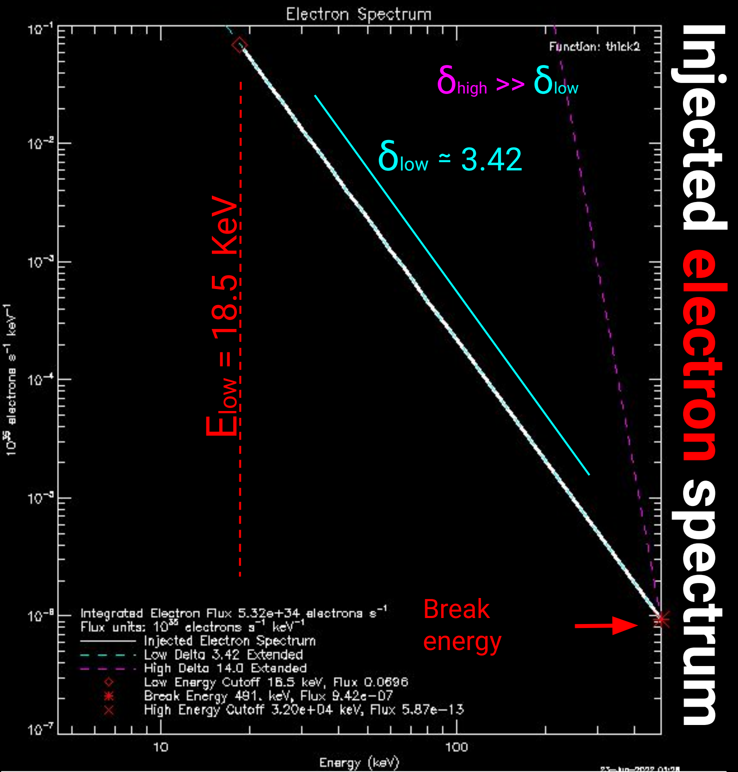

Adapted from Lin , Hudson 1976

Thick-target bremsstrahlung photon production

$$\frac{dQ}{d(h\nu)} = \int_0^\infty dE \frac{d\sigma}{d(h\nu)}(E, h\nu) \left(\frac{dE}{d\xi}\right)^{-1} f\eta \int_E^\infty \frac{dN}{dE'} dE',$$

HXR photons per energy unit | differential cross-section | energy loss | ion density of target | electron spectrum

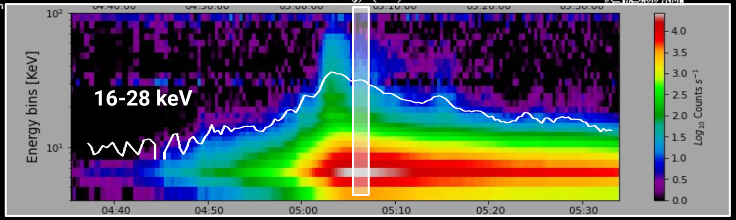

Radio Diagnostics: Frequency Drift Rate

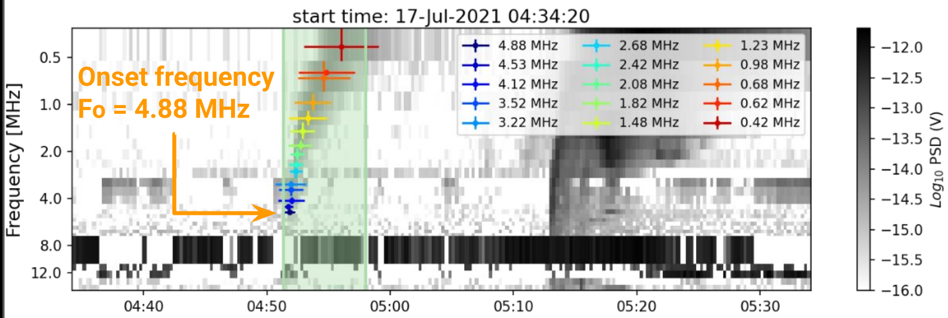

Given a **ne (r) model**, the onset frequency **Fo** can be associated with an heliocentric distance

F_o = 4.88 MHz
R_o = 2.76 R⊙

$$\frac{df}{dt} = \frac{\partial f}{\partial n_e}\frac{\partial n_e}{\partial r}\frac{\partial r}{\partial t}$$

Freq. drift rate | **Exciter Velocity (v)**

Electron density **ne [cm-3]** decreases with heliocentric distance **r [R⊙]** (Leblanc,1998)

$$n_e(r) = 8.0 \times 10^7 r^{-6} + 4.1 \times 10^6 r^{-4} + 3.3 \times 10^5 r^{-2}$$

Plasma emission frequency **fp [kHz]** depends on electron density **ne [cm-3]**

$$f_p \approx 9 \times \sqrt{n_e}$$

EM waves can be emitted at the **fundamental** (**fp**) and harmonic component (~2 **fp**)

Fitting the time profiles for each frequency channel with a **parametric model** can provide the **peak and onset** of emission per frequency

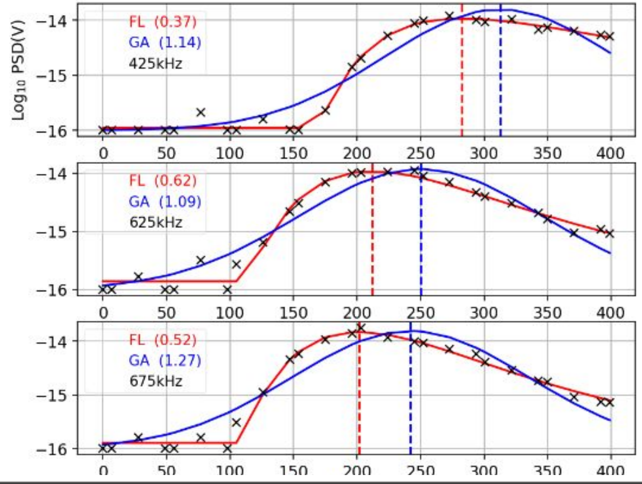

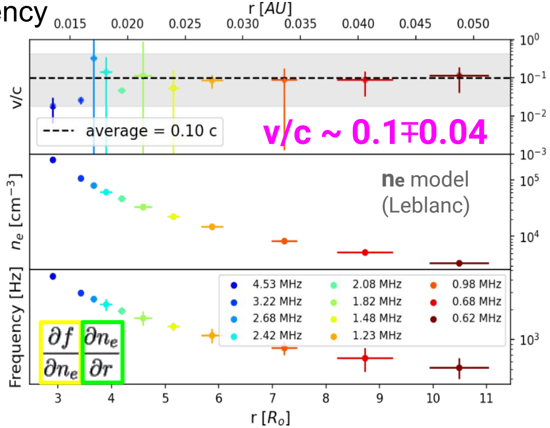

Calculating **df/dt** from data, estimating **dr/dt** with models

A work in progress: Paper on November 2020 events

- **Continue the observation of X-ray flares in the November 2020 period**
  - same active region? what is different?
- **Integrate the frequency drift analysis and spectroscopy to the study of these flares**
  - what can we say about the energy content of the accelerated electrons? any relation with appearance of IPT3?
- **Use data of other instruments when possible**
  - EUI FSI 174/304 A
  - in-situ particle detections with EPD
  - Ground-based Radio
- **Robust statistical analysis with a larger population of events**